Effect of Nonstoichiometry on the Structure and Microwave Dielectric Properties of $Ba(Mg_{0.33}Ta_{0.67})O_3$

Kuzhichalil P. Surendran,[†] Mailadil T. Sebastian,*,[†] Pezholil Mohanan,[‡] Roberto L. Moreira,[§] and Anderson Dias[||]

Ceramic Technology Division, Regional Research Laboratory, Trivandrum 695 019, India, Department of Electronics, Cochin University of Science and Technology, Cochin 682 022, India, Departamento de Física, ICEX, UFMG, C.P. 702, Belo Horizonte-MG 30123-970, Brazil, and Departamento de Engenharia Metalúrgica e de Materiais, UFMG, Rua Espírito Santo 35, Sala 206, Belo Horizonte-MG 30160-030, Brazil

Received September 14, 2004. Revised Manuscript Received October 7, 2004

The effect of a slight A- and B-site cation nonstoichiometry on the structure, densification, and microwave dielectric properties of $Ba(Mg_{1/3}Ta_{2/3})O_3$ (BMT) was investigated. Magnesium and barium nonstoichiometric compositions based on $Ba(Mg_{0.33-x}Ta_{0.67})O_3$ [$x = -0.015, -0.010, -0.005, 0.0, 0.005, 0.010, 0.015, 0.020, 0.025$, and 0.030] and $Ba_{1-x}(Mg_{0.33}Ta_{0.67})O_3$ [$x = -0.015, -0.010, -0.005, 0.0, 0.0025, 0.005, 0.0075, 0.010, 0.015, 0.020, 0.025$, and 0.030] were prepared using the conventional solid-state ceramic route. The lattice distortion and cation ordering were determined using X-ray diffraction technique. The phase composition and surface morphology were studied by EDX and scanning electron microscopy techniques, respectively. The sintered samples were characterized in the microwave frequency range using the resonance technique. It is found that a slight barium or magnesium deficiency can improve density, microwave dielectric properties, and cation ordering, while the addition of excess ions deteriorated them. The improvement in microwave dielectric properties was more pronounced in barium nonstoichiometric samples. Microwave dielectric properties of $Ba_{0.9925}(Mg_{0.33}Ta_{0.67})O_3$ [$\epsilon_r = 24.7$, $\tau_f = 1.2$ ppm/°C, $Q_u xf = 152\,580$ GHz] and $Ba(Mg_{0.3183}Ta_{0.67})O_3$ [$\epsilon_r = 25.1$, $\tau_f = 3.3$ ppm/°C and $Q_u xf = 120\,500$ GHz] were found to be better than stoichiometric BMT [$\epsilon_r = 24.2$, $\tau_f = 8$ ppm/°C and $Q_u xf = 100\,500$ GHz]. Raman spectroscopy was employed to study the effects of nonstoichiometry and related lattice distortions in BMT ceramics on their vibrational modes. Raman results clearly showed the 1:2 ordered structures of these materials with all active modes assigned. The spectra showed variations in the normal modes as a function of the composition. Also secondary phases contributed to the changes in the Raman spectra observed in compounds with $x \geq 0.02$.

Introduction

Complex perovskite oxides based on $Ba(B'_{1/3}B''_{2/3})O_3$ [B′ = Mg, Zn; B″ = Ta, Nb] are reported to be ideal for dielectric resonator (DR) applications due to their high dielectric constant, high unloaded quality factor, and low variation of the resonant frequency with temperature.[1] These are vitally important requirements for a solid-state component to be used in key microwave devices such as filters and oscillators used in telecommunication industry. Among the Ba-based complex perovskites, $Ba(Mg_{1/3}Ta_{2/3})O_3$ (BMT) has stimulated a surge of interest for its excellent dielectric properties in the *X* band (8−12 GHz) and is considered to be the archetypal high-*Q* DR material.[2] Galasso and Pyle[3] found that it crystallizes in a disordered cubic structure or in an ordered hexagonal structure. The ordered structure results from the 1:2 ordering of the B′ and B″ cations along the ⟨111⟩ direction of the cubic perovskite unit cell. It is well-established that B-site ordering in complex perovskites has a significant influence in the dielectric losses at microwave frequencies. Rapid firing and doping[4] are some of the techniques adopted to improve sinterability and dielectric properties of BMT.

One method to improve the sinterability of the ceramic is to enhance the material transport processes in the dielectric by altering the material's stoichiometry. Historically, Desu and O'Bryan[5] made the first attempt in correlating the phenomenon of the excellent microwave quality factor of a prominent complex perovskite candidate $Ba(Zn_{1/3}Ta_{2/3})O_3$ (BZT) with B-site cation nonstoichiometry. They explained the low-loss property on the basis of ZnO evaporation. The duo postulated that the escape of ZnO from the sample leads to crystallographic distortion, which in turn may promote

* Corresponding author. Telephone: +91 471 2515294. Fax: +91 471 2491712. E-mail: mailadils@yahoo.com.
† Regional Research Laboratory.
‡ Cochin University of Science and Technology.
§ Departamento de Física, UFMG.
|| Departamento de Engenharia Metalúrgica e de Materiais, UFMG.

(1) Wersing, W. In *Electronic Ceramics*; Steele, B. C. H., Ed.; Elsevier Applied Science: London, U.K., 1991.
(2) Moulson, A. J.; Herbert, J. M. *Electroceramics*; Chapman and Hall: London, U.K., 1990; Chapter 5.
(3) Galasso, F. S.; Pyle, R. *J. Phys. Chem.* **1963**, *67*, 482.
(4) Yoon, K. H.; Kim, J. B.; Kim, E. S. *Ceramics—Charting the Future, Proceedings of the 8th CIMTEC*, Florence, Italy, June 28−July 4, 1994; Technica Socit a responsibit limitat Faenza, 1995; pp 2543−50.
(5) Desu, S. B.; O'Bryan, H. M. *J. Am. Ceram. Soc.* **1985**, *68*, 546.

10.1021/cm048411s CCC: $30.25 © 2005 American Chemical Society
Published on Web 12/07/2004

1:2 ordering. This investigation was further extended by Kawashima,[6] who found that inhomogeneous densification was achieved by ZnO evaporation and can be compensated by muffling in ZnO (the quality factor decreased). Subsequently in 1996, Choi et al.[7] revisited this problem in BZT using transmission electron microscopy (TEM) and observed a new type of ordering along the ⟨110⟩ direction, apart from the formation of $Ba_{0.5}TaO_3$ and $Ba_3TaO_{5.5}$ phases in zinc deficient samples. The effect of a slight nonstoichiometry and chemical inhomogeneity on the order−disorder phase transformation has also been studied[8] in $Ba(Ni_{1/3}Nb_{2/3})O_3$ and $Ba(Zn_{1/3}Nb_{2/3})O_3$. In another significant attempt, Paik et al.[9] investigated the effect of Mg deficiency on the microwave dielectric properties of complex perovskite $Ba(Mg_{0.33}Nb_{0.67})O_3$. These authors claimed an improvement in density and unloaded Q factor for $x = 0.02$ in $Ba(Mg_{0.33-x}Nb_{0.67})O_3$, which was explained to be due to enhanced grain boundary mass transport generated by lattice defects. It may be noted that the volatilization of MgO in $Ba(Mg_{1/3}Ta_{2/3})O_3$ at high temperature leads[10] to the formation of secondary phases. Later on, Tochi[11] observed that the sinterability of BMT could be improved with the addition of the extra phase $BaTa_2O_6$ that formed during calcination. It was also reported[12] that, among the three starting materials, the reactivity of MgO is inferior to $BaCO_3$ and Ta_2O_5. In the conventional sintering processes, the reaction between the latter two give rise to Ba−Ta−O satellite phases, which is detrimental to the microwave dielectric properties of the ceramic.[13] An improvement in the degree of 1:2 ordering and sinterability was proposed by Lu and Tsai[14] in Ba-deficient $Ba(Mg_{1/3}Ta_{2/3})O_3$ ceramics, but they did not study the effects of A-site cation deficiency on the microwave dielectric properties of BMT. The effect of Mg deficiency on the microwave dielectric properties of BMT was also investigated by a couple of research groups[15,16] who found that the Mg-deficient specimen showed faster rate of grain growth than stoichiometric BMT. However, nonstoichiometric samples showed lower Q values.

The brief discussion made above suggests that the effect of B-site deficiency improves the dielectric properties in $Ba(Zn_{1/3}Ta_{2/3})O_3$, while it is detrimental to the dielectric quality factor in $Ba(Mg_{1/3}Ta_{2/3})O_3$. This drew our special attention into the complex relationship between stoichiometry and microwave loss quality of complex perovskite $Ba(Mg_{1/3}Ta_{2/3})O_3$ ceramics. In this research paper, the effect of Ba and Mg nonstoichiometries on the densification, microstructure, structural ordering, and microwave dielectric properties of $Ba(Mg_{1/3}Ta_{2/3})O_3$ is investigated. The effects of nonstoichiometry and associated lattice distortion on the vibrational modes are studied by laser Raman scattering.

Experimental Section

Ceramic Preparation. The nonstoichiometric compositions based on $Ba(Mg_{0.33-x}Ta_{0.67})O_3$ [$x = -0.015$, -0.010, -0.005, 0.0, 0.005, 0.010, 0.015, 0.020, 0.025, and 0.030] and $Ba_{1-x}(Mg_{0.33}Ta_{0.67})O_3$ [$x = -0.015$, -0.010, -0.005, 0.0, 0.0025, 0.005, 0.0075, 0.010, 0.015, 0.020, 0.025, and 0.030] were prepared by the conventional solid-state ceramic route. High-purity (>99.9%) powders of $BaCO_3$ (Aldrich), $(MgCO_3)_4{\cdot}Mg(OH)_2{\cdot}5H_2O$ (Aldrich), and Ta_2O_5 (Nuclear Fuel Complex, India) were used as starting materials. It has been previously reported[17] that the processing temperature of stoichiometric $Ba(Mg_{0.33}Ta_{0.67})O_3$ could be appreciably reduced by using $(MgCO_3)_4{\cdot}Mg(OH)_2{\cdot}5H_2O$ instead of MgO or $MgCO_3$. The powders were weighed in appropriate molar ratio and ball milled in a polyethylene mill bottle with zirconia balls for 24 h, using distilled water as the mixing medium. The slurry was dried at 100 °C in a hot-air oven and was calcined in platinum crucibles at 1300 °C for 10 h in air with intermediate grinding. The calcined powder was ground in an agate mortar for several hours, and then 3 wt % poly(vinyl alcohol) was added as binder. The slurry was mixed up, dried, and again ground for 1 h. It is then made into cylindrical compacts of about 14 mm diameter and 6−8 mm length in a tungsten carbide (WC) die under a pressure of about 150 MPa to maintain an aspect ratio (D/L) of 2. These compacts were fired at a rate of 5 °C/min up to 500 °C and soaked at 500 °C for 1 h to expel the binder. The pellets were sintered at 1600 °C for 4 h in air on platinum plates at a heating rate of 10 °C/min. After sintering, the samples were allowed to cool to room temperature at the rate of 1 °C/ min. The well-polished ceramic pellets were used for microwave measurements. The bulk densities of the sintered samples were measured using Archimedes's method. The error in measurement of the bulk density was less than 0.1%. The cation ordering and lattice distortion were analyzed by an X-ray diffractometer (Rigaku-Dmax 1C, Japan) using Cu Kα radiation. The lattice parameters were determined as the average of the values calculated from the prominent reflections of powder diffraction. The error in lattice parameter was calculated using the root sum of squares (RSS) method. The surface morphology of the sintered and thermally etched samples was analyzed using a scanning electron microscope (SEM S-2400, Hitachi, Japan). The stoichiometry of the samples was measured using the SEM/EDX facility with Oxford ISIS software.

Microwave Characterization. The dielectric properties such as dielectric constant ϵ_r and quality factor Q_u of the dielectric materials were measured in the microwave frequency range by using a vector network analyzer HP 8510 C, HP 8514 test unit, and HP 8341 B sweep oscillator. ϵ_r was measured by the postresonator method of Hakki and Coleman,[18] using the $TE_{01\delta}$ mode of resonance coupled through E-field probes. The accuracy of ϵ_r measurement is restricted to the accuracy in measurement of resonant frequency and dimensions of the sample. The error in ϵ_r measurement was typically less than ±0.01. Usually, three samples were prepared in a batch corresponding to a particular composition and the measurements were made at least twice per each specimen. The unloaded quality factor was measured by the resonance method using a tunable copper cavity whose interior was coated with silver.[19] The ability to tune the frequency is very useful for the accurate determination

(6) Kawashima, S. *Am. Ceram. Soc. Bull.* **1993**, *72*, 120.
(7) Choi, S. J.; Nahm, S.; Kim, M. H.; Byun, J. D. *Korean J. Ceram.* **1996**, *2*, 242.
(8) Hong, K. S.; Kim, I. T.; Yoon, S. J. *J. Mater. Sci.* **1995**, *30*, 514.
(9) Paik, J. H.; Nahm, S.; Byun, J. D.; Kim, M. H.; Lee, H. J. *J. Mater. Sci. Lett.* **1998**, *17*, 1777.
(10) Yang, C.; Zhou, D.; Huang, C.; Qin, G. *J. Adv. Mater.* **1998**, *31*, 8.
(11) Tochi, K. *J. Ceram. Soc. Jpn.* **1992**, *100*, 1464.
(12) Kusumoto, K.; Sekiya, T. *Mater. Res. Bull.* **1998**, *33*, 1367.
(13) Fang, Y.; Hu, A.; Ouyang, S.; Oh, J. J. *J. Eur. Ceram. Soc.* **2001**, *21*, 2745.
(14) Lu, C.-H.; Tsai, C.-C. *J. Mater. Res.* **1996**, *5*, 1219.
(15) Byun, J. B.; Nahm, S.; Lee, D. W.; Kim, Y. S.; Kim, M. H.; Lee, H. J. *Proceedings of the 9th International Meeting on Ferroelectricity*, Seoul, Korea; Korean Physical Society: Seoul, Korea, 1997; pp 24−29.
(16) Lee, J.-A.; Kim, J.-J.; Lee, H.-Y.; Kim, T.-H.; Choy, T.-G. *J. Korean Ceram. Soc.* **1994**, *31*, 1299.
(17) Chen, X. M.; Wu, Y. J. *Mater. Lett.* **1996**, *26*, 237.
(18) Hakki, B. W.; Coleman, P. D. *IRE Trans. Microwave Theory Tech.* **1960**, *MTT-8*, 402.

of the resonant mode and to allow it to measure samples with various dimensions. Also the electric field is symmetric with the geometry of the sample and cavity, which helps to reduce the sources of loss due to cavity. The sample was isolated using a quartz spacer, from the effects of losses due to the finite resistivity of the cavity. The cavity was weakly coupled so that errors of insertion loss due to the uncertainty of the cable loss does not contribute to an error in the unloaded quality factor. The coefficient of thermal variation of resonant frequency τ_f was measured by noting the temperature variation of the resonant frequency of the $TE_{01\delta}$ mode in the reflection configuration, over the range of temperature of 25−80 °C, keeping the dielectric in the end-shorted position.

Raman Spectroscopy. Micro-Raman scattering spectra were recorded using a Jobin-Yvon LABRAM-HR spectrometer, equipped with an 1800 grooves/mm diffraction grating, a liquid-N_2-cooled CCD detector, and a confocal microscope (100× objective). The experimental resolution was better than 1 cm^{-1}. After fitting, the ultimate resolution was 0.2 cm^{-1}. The measurements were carried out in backscattering geometry at room temperature, using the 632.8 nm line of a helium−neon ion laser (power, 12.5 mW) as excitation source. A holographic notch filter was used to stray light rejection (Rayleigh scattered light). The sample surfaces of the sintered materials were previously polished to an optical grade in order to improve the ratio of inelastic to elastic scattered light. The normal modes in these perovskites are sensitive to the presence of disordering and local stresses promoted by atomic substitution and/or nonstoichiometry.

Results and Discussion

The most efficient way of reducing the dielectric loss is the formation of 1:2 long-range ordered clusters.[20] In the ordered form (space group $P\bar{3}m1$), the Mg^{2+} and Ta^{5+} cations are distributed on individual ⟨111⟩ planes of the perovskite subcell with alternating {Mg,Ta,Ta} sequence. This results in the appearance of superstructure reflections at $[h \pm 1/3, k \pm 1/3, l \pm 1/3]$ positions. In the disordered phase, Mg^{2+} and Ta^{5+} cations are randomly distributed on the octahedral sites of the perovskite subcell, which causes a change in symmetry to cubic (space group $Pm3m$). The cation ordering parameter for BMT can be calculated using the following equation

$$S = \sqrt{\frac{(I_{(100)}/I_{(110),(102)})_{obsd}}{(I_{(100)}/I_{(110),(102)})_{theor}}} \qquad (1)$$

where the theoretical value of the ratio of the integral intensity of super structural reflection line (100) to that of the (110,102) line, $(I_{100}/I_{110,102})_{theor}$, is 8.3%, putting all the atoms in approximate ideal positions in BMT crystal lattice. Lu and Tsai[14] later modified this ratio to 8.14%. The accurate determination of the cation order parameter must be done through Rietveld refinement technique, which is beyond the scope of this investigation. However, in a real case, the structure factors of major reflections (function of ions located in crystal structure) vary with slight deviations of cations from their ideal high-symmetry positions. The recent structural analysis carried out by Janaswamy et al.[21] and Lufaso[22]

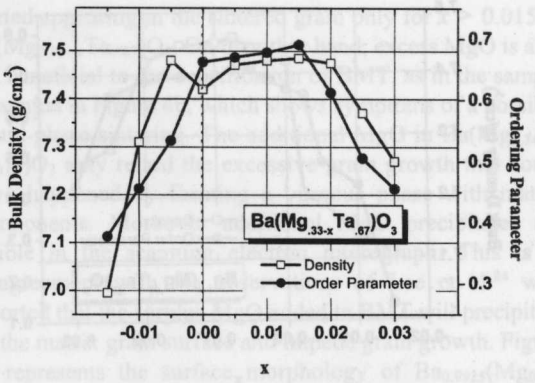

Figure 1. Variation of bulk density and order parameter of $Ba(Mg_{0.33-x}Ta_{0.67})O_3$, vs x.

suggest that a more accurate value for $(I_{100}/I_{110,102})_{theor}$ is equal to 8.7%. This value has been used for the determination of the order parameter in this study. The error in the calculation of the ordering parameter was less than ±0.001.

A slight stoichiometric deviation of Mg can bring about two effects in the ceramic: (i) appearance of additional phase, such as $BaTa_2O_6$ and $Ba_5Ta_4O_{15}$; (ii) improvement of the sinterability by bulk diffusion due to vacancies created by MgO loss. The bulk density of BMT is more or less invariant with Mg deficiency up to $x = 0.02$ in $Ba(Mg_{0.33}Ta_{0.67})O_3$, as shown in Figure 1. The densification reaches a maximum value of 7.485 g/cm³ for $x = 0.015$ in $Ba(Mg_{0.33-x}Ta_{0.67})O_3$, which is about 98% of the theoretical density (7.625 g/cm³) of stoichiometric BMT. For higher values of x ($x > 0.02$ in $Ba(Mg_{0.33-x}Ta_{0.67})O_3$) the density decreases due to the formation of additional phases such as $BaTa_2O_6$ and $Ba_5Ta_4O_{15}$. In addition to that, it has been well-established[23] that a large extent of nonstoichiometry results in lattice distortion, which can hinder the diffusion mechanism for densification. In our investigation the density is slightly higher for $x = -0.005$ than pure BMT. The higher percentage of excess MgO ($x > -0.05$ in $Ba(Mg_{0.33-x}Ta_{0.67})O_3$) would remain in the grain boundary and significantly hinder the diffusion mechanism and the migration of grain boundary, thereby decreasing the density of the specimen. It must be noted that the densification mechanism and cation ordering phenomenon do not bear a one-to-one correspondence in Mg nonstoichiometric compositions. The cation ordering (see Figure 1), which is a microscopic phenomenon, reaches its maximum value (0.69) for $x = 0.015$ in $Ba(Mg_{0.33-x}Ta_{0.67})O_3$, while ordering is poor for pure and Mg excess specimens.

The evolution of density and cation ordering in Ba nonstoichiometric BMT is given in Figure 2. The sintered specimens showed a trend of densification in slightly Ba deficient samples. The bulk density is maximum (7.459 g/cm³, which is about 97.8% of the X-ray density of stoichiometric BMT sample) for $x = 0.0075$ in $Ba_{1-x}(Mg_{0.33}Ta_{0.67})O_3$. The density is decreased as the barium content is decreased below $x = 0.02$ in $Ba_{1-x}(Mg_{0.33}Ta_{0.67})O_3$, which can be attributed to the formation of additional phases such as $MgTa_2O_6$. A similar

(19) Krupka, J.; Derzakowski, K.; Riddle, B.; Jarvis, J. B. *Meas. Sci. Technol.* **1998**, *9*, 1751.
(20) Junichi, K. *Seramikkusu* **1992**, *27*, 728.
(21) Janaswamy, S.; Murthy, G. S.; Dias, E. D.; Murthy, V. R. K. *Mater. Lett.* **2002**, *55*, 414.
(22) Lufaso, M. W. *Chem. Mater.* **2004**, *16*, 2148.
(23) Burdett, J. K.; Mitchell, J. F. *Prog. Solid State Chem.* **1995**, *23*, 131.

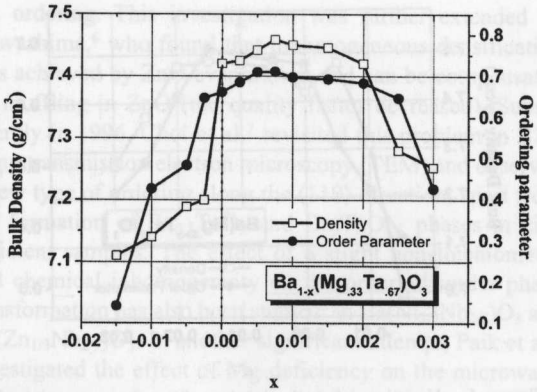

Figure 2. Variation of bulk density and order parameter of $Ba_{1-x}(Mg_{0.33}Ta_{0.67})O_3$, vs x.

observation in nonstoichiometric BMT was reported by Lu and Tsai,[14] who found an increase in densification for $x = -0.005$ in $Ba_{1+x}(Mg_{0.33}Ta_{0.67})O_3$. The samples with surplus Ba content show poor densification. This result is consistent with the similar observation made in $Ba(Zn_{0.33}Ta_{0.67})O_3$ by Kawashima,[12] who observed a degradation in the shrinkage of BZT samples with excess Ba content. The cation ordering parameter shows reasonably better values in Ba-deficient samples in comparison with Mg-deficient ones. The ordering parameters for $x = 0.0$, 0.0025, 0.005, 0.0075, and 0.01 are 0.66, 0.685, 0.709, 0.711, and 0.697, respectively. On the other hand, the addition of excess Ba ions damages the 1:2 cation ordering (see Figure 2).

In this investigation, it was found that one composition each in Mg- and Ba-deficient perovskites [$Ba(Mg_{0.3183}Ta_{0.67})O_3$ and $Ba_{0.9925}(Mg_{0.33}Ta_{0.67})O_3$] have exhibited excellent properties. It must be noted that the cation nonstoichiometry in $Ba(Mg_{0.33}Ta_{0.67})O_3$ is compensated for as a manifestation of the oxygen anion concentration in BMT lattice. So the more appropriate representations of the nonstoichiometric BMT are $Ba(Mg_{0.33-x}Ta_{0.67})O_{3\pm\delta}$ and $Ba_{1-x}(Mg_{0.33}Ta_{0.67})O_{3\pm\delta}$, where δ determines the oxygen nonstoichiometry which can be determined using semiempirical methods.[24,25] Even though this oxygen nonstoichiometry has drastic effects on the dielectric properties, we avoid the representation of nonstoichiometric BMT for the sake of simplicity.

The XRD patterns of typical Mg-deficient, Ba-deficient, and stoichiometric $Ba(Mg_{0.33}Ta_{0.67})O_3$ are given in Figure 3. The presence of superstructure reflections is visible in the powder X-ray pattern recorded from pure BMT. As the Mg deficiency is increased to $x = 0.015$ in $Ba(Mg_{0.33-x}Ta_{0.67})O_3$ (see Figure 3, curve c), the intensity of 1:2 superstructure lines increases, but no traces of any additional phases are visible, within the limits of experimental error. But a larger level of Mg deficiency $x > 0.015$ will initiate the formation of additional phases like[26] $BaTa_2O_6$ and $Ba_5Ta_4O_{15}$,[27,28] whose presence is reported to deteriorate the dielectric quality factor

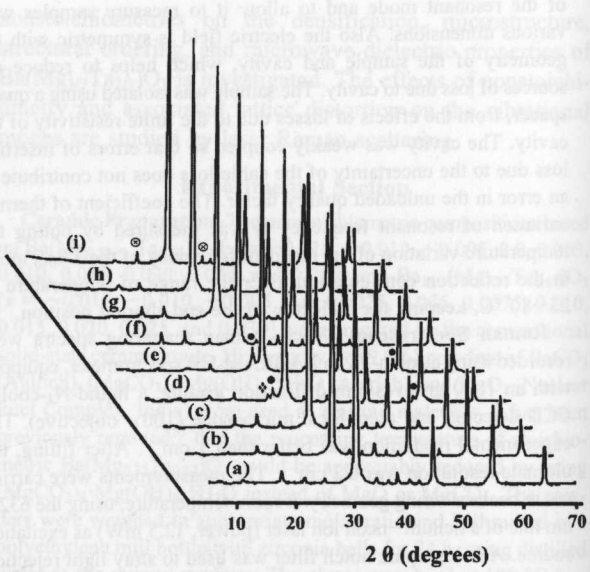

Figure 3. Powder diffraction patterns of some typical nonstoichiometric compositions of BMT: (a) pure $Ba(Mg_{0.333}Ta_{0.667})O_3$; (b) $Ba(Mg_{0.3233}Ta_{0.667})O_3$; (c) $Ba(Mg_{0.3183}Ta_{0.667})O_3$; (d) $Ba(Mg_{0.3133}Ta_{0.667})O_3$; (e) $Ba(Mg_{0.3033}Ta_{0.667})O_3$; (f) 0.9925 $Ba(Mg_{0.333}Ta_{0.667})O_3$; (g) 0.99 $Ba(Mg_{0.333}Ta_{0.667})O_3$; (h) 0.98 $Ba(Mg_{0.333}Ta_{0.667})O_3$; (i) 0.97$Ba(Mg_{0.333}Ta_{0.667})O_3$. Filled circles represent $Ba_5Ta_4O_{15}$, the dotted diamond is for $BaTa_2O_6$, and circled × are for $MgTa_2O_6$.

in BMT. The escape of the B″ site ion in 1:2 type Ba-based complex perovskites may result in formation of additional phases like[29,30] $Ba(B'_{1/8}B''_{3/4})O_3$ whose crystal structure has been reported by Abakumov et al.[31] Recently, Davies et al.[32] confirmed the formation of $Ba_8ZnTa_6O_{24}$ in Zn-deficient $Ba(Zn_{0.33}Ta_{0.67})$ dielectrics. This compound has a hexagonal perovskite structure (space group $P6_3cm$) with an eight-layer $(cchc)_2$ close-packed arrangement of BaO_3 layers. In a separate investigation, Bieringer et al.[33] also explored the nonstoichiometry and ordered domain growth aspects of zinc deficient BZT in light of the newly formed complex perovskite $Ba_8ZnTa_6O_{24}$ phase. But the present study does not favor the formation of a possible compound like $Ba_8MgTa_6O_{24}$ in Mg-deficient perovskites. On the hand the X-ray diffractogram of typical Ba-deficient BMT ceramics (see Figure 3, curves f–i) shows comparatively better cation ordering of B-site cations, which is evidenced by the appearance of discrete $\pm 1/3\{hkl\}$ superlattice reflections perpendicular to, e.g., $\langle 111\rangle$ and $\langle 11\bar{1}\rangle$. The samples are free of additional phases for $x \leq 0.025$. However, decreasing the barium concentration below a threshold level will result in the formation of additional phases such as $MgTa_2O_6$ (see Figure 3, curve i).

Figure 4 presents the scanning electron micrographs of three nonstoichiometric specimens sintered at 1600 °C. The

(24) Lee, J.-A.; Kim, J.-J.; Lee, H.-Y.; Kim, T.-H.; Choy, T.-G. *J. Korean Ceram. Soc.* **1994**, *31*, 1561.
(25) Yang, Z.; Lin, Y. S. *Solid State Ionics* **2002**, *150*, 245.
(26) Sugiyama, M.; Inuzuka, T.; Kubo, H. *Ceram. Trans.* **1990**, *15*, 153.
(27) Liang, M.-H.; Hu, C.-T.; Chiou, C.-G.; Tsai, Y.-N.; Lin, I.-N. *Jpn. J. Appl. Phys.* **1999**, *38*, 5621.
(28) Lin, I.-N.; Liang, M.-H.; Hu, C.-T.; Steeds, J. *J. Eur. Ceram. Soc.* **2001**, *21*, 1705.
(29) Tolmer, V.; Desgardin, G. *J. Am. Ceram. Soc.* **1997**, *80*, 1981.
(30) Reaney, I. M.; Wise, P. L.; Qazi, I.; Miller, C. A.; Price, T. J.; Cannell, D. S.; Iddles, D. M.; Rosseinsky, M. J.; Moussa, S. M.; Bieringer, M.; Noailles, L. D.; Ibberson, R. M. *J. Eur. Ceram. Soc.* **2003**, *23*, 3021.
(31) Abakumov, A. M.; Tendeloo, G. V.; Scheglov, A. A.; Shpanchenko, R. V.; Antipov, E. V. *J. Solid State Chem.* **1996**, *125*, 102.
(32) Davies, P. K.; Borisevich, A.; Thirumal, M. *J. Eur. Ceram. Soc.* **2003**, *23*, 2461.
(33) Bieringer, M.; Moussa, S. M.; Noailles, L. D.; Burrows, A.; Kiely, C. J.; Rosseinsky, M. J.; Ibberson, R. M. *Chem. Mater.* **2003**, *15*, 586.

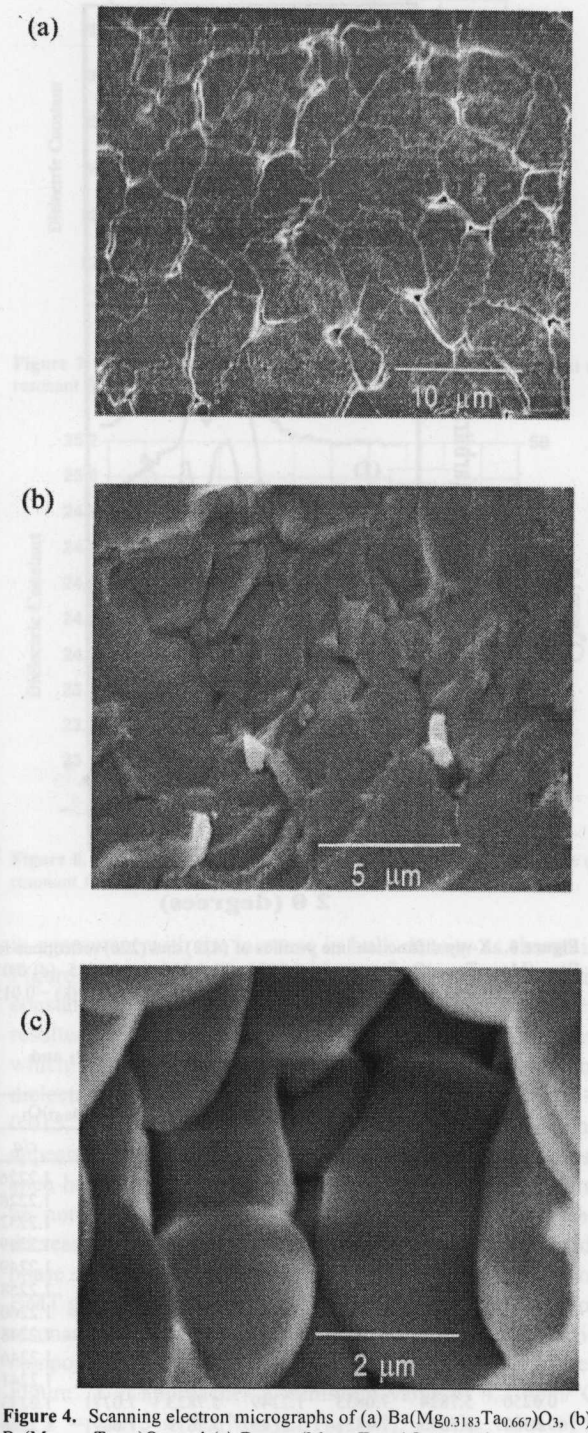

Figure 4. Scanning electron micrographs of (a) $Ba(Mg_{0.3183}Ta_{0.667})O_3$, (b) $Ba(Mg_{0.3483}Ta_{0.67})O_3$, and (c) $Ba_{0.9925}(Mg_{0.33}Ta_{0.67})O_3$ ceramics.

surface morphology recorded from a typical Mg-deficient BMT [$Ba(Mg_{0.3183}Ta_{0.667})O_3$] sample is given in Figure 4a. There have been previous reports[25] showing that grain growth will be more rapid in Mg-deficient BMT ceramics, consequent to the formation of sandwich-type precipitates of $Ba_5Ta_4O_{15}$ within the matrix grain. Here also it is evident that the average size of BMT grain is about 5−8 μm in Mg-deficient specimens, with reasonably good close packing of grains. It must be remembered that in our experiment the additional phases such as $BaTa_2O_6$ and $Ba_5Ta_4O_{15}$ have started appearing in the sintered grain only for $x > 0.015$ in $Ba(Mg_{0.33-x}Ta_{0.67})O_3$. On the other hand, excess MgO is also not beneficial to the densification of BMT, as in the sample presented in Figure 4b, which shows symptoms of a possible liquid-phase sintering. The additional MgO in $Ba(Mg_{0.3483}Ta_{0.67})O_3$ may retard the excessive grain growth that could have happened by forming a vitreous phase with matrix components. Moreover additional MgO precipitates are visible in the scanning electron micrograph. This is in disagreement with the observations of Lee et al.[24] who reported that the surplus MgO added to BMT will precipitate on the matrix grain surface and impede grain growth. Figure 4c represents the surface morphology of $Ba_{0.9925}(Mg_{0.33}Ta_{0.67})O_3$ which is taken from a fractured surface. Here, no additional phases are visible in the SEM picture, and the grain size is around 2−3 μm. A previous report[14] on the Ba-deficient BMT ceramics observed the presence of magnesium-rich small darker grains, which appeared as a solidified liquid. But no evidence of liquid-phase sintering was revealed in our Ba-deficient BMT samples.

Since the sintering occurs through mass transport and the rate of mass transport depends on the defect mechanism of ionic crystals, the crystal defect occurring even at the time of calcination can control the sintering behavior of BMT. Based on the powder diffraction analysis, three cases can be considered for the dominant defect types in calcined BMT powder: (i) A-site vacancy is the major defect, (ii) B-site (B′ or B″) vacancy is the major defect, and (iii) both A- and B-site vacancies occur simultaneously. One of these cases plays a major role during the sintering process.[34] In complex perovskite $Ba(Zn_{1/3}Ta_{2/3})O_3$ (BZT) ceramics, Desu and O'Bryan[5] observed that prolonged sintering up to 100 h increased the unloaded quality factor which was due to a more complete ordering of Mg and Ta. This ordering results in the expansion of the unit cell along the body diagonal ⟨111⟩ direction and in the splitting of the (422) and (226) powder diffraction peaks. Hence, it is expected that the B′ ion nonstoichiometry may have a vital role on the sinterability and microwave dielectric properties of $Ba(B'_{1/3}Ta_{2/3})O_3$ [B′ = Mg, Zn]. The splitting of the profiles of (422) and (266) reflections due to the lattice distortion of nonstoichiometric $Ba(Mg_{0.33-x}Ta_{0.67})O_3$ and $Ba_{1-x}(Mg_{0.33}Ta_{0.67})O_3$ for different values of x is shown in Figures 5 and 6, respectively. The XRD patterns shown in Figure 5 were recorded with a slow scan of $2\Theta = 1°$/min. The splitting of the peaks is associated with cation ordering, which has both kinetic and thermodynamic parts. Cation ordering is slow in these perovskites and is accomplished by very prolonged heat treatment. At 1600 °C, the temperature is sufficient to attain a highly ordered perovskite; however, the sintering time (4 h) is insufficient to reach equilibrium cation order conditions at that temperature. Slow cooling assists in the ordering but does not guarantee the presence of equilibrium ordering. Changes in composition, which kinetically assists cation ordering, are being followed in this experiment. In general, small amounts of cation vacancies facilitate cation ordering, which agrees with the results of the present study.[9] For stoichiometric BMT the profiles of (422) and (226) reflec-

(34) Youn, H. J.; Kim, H. Y.; Kim, H. *Jpn. J. Appl. Phys.* **1996**, *35*, 3947.

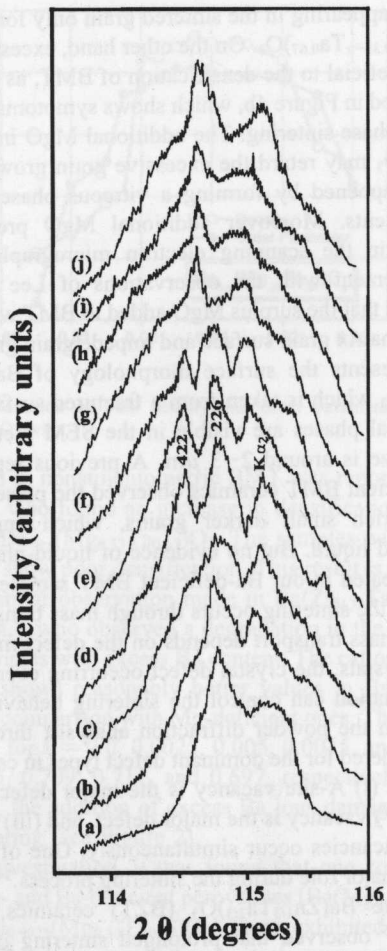

Figure 5. X-ray diffraction line profiles of (422) and (226) reflections for $Ba(Mg_{0.33-x}Ta_{0.67})O_3$ for x = (a) 0.03, (b) 0.025, (c) 0.02, (d) 0.015, (e) 0.01, (f) 0.005, (g) 0.0, (h) −0.005, (i) −0.010, and (j) −0.015.

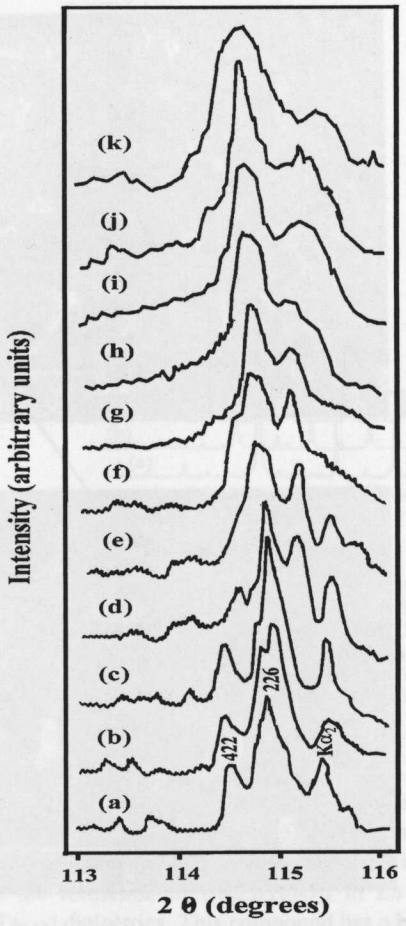

Figure 6. X-ray diffraction line profiles of (422) and (226) reflections for $Ba_{1-x}(Mg_{0.33}Ta_{0.67})O_3$ for x = (a) 0.0025, (b) 0.005, (c) 0.0075, (d) 0.01, (e) 0.015, (f) 0.02, (g) 0.025, (h) 0.03, (i) −0.005, (j) −0.01, and (k) −0.015.

tions are not distinguishable from the standard $K\alpha_2$ line, which has apparently no lattice distortion. It is observed that splitting is more pronounced for $x = 0.015$ in $Ba(Mg_{0.33-x}Ta_{0.67})O_3$ (see curve d in Figure 5). A similar phenomenon was observed in Ba-deficient complex perovskites, where the maximum line splitting was observed for $x = 0.0075$ in $Ba_{1-x}(Mg_{0.33}Ta_{0.67})O_3$ (see Figure 6). It is interesting to note that the line splitting is in accordance with the rise and fall of the ordering parameter as shown in Figures 1 and 2. The splitting of the (422) and (226) reflections occur at the maximum of the order parameter.

The ordering of Mg and Ta ions results in the expansion of the original unit cell along the ⟨111⟩ direction[35] so that the value of c/a assumes a value greater than $\sqrt{(3/2)} = 1.22474$. It is interesting to note that the value of the cell parameter c also increases from 7.0699 to 7.0845 Å when x changes from 0.0 to 0.015 and the cell parameter ratio c/a increases up to $x = 0.015$ (Table 1). On the other hand, the lattice parameter ratio is smallest for MgO-deficient samples. In Ba-deficient samples the c/a ratio increases with x and reaches a maximum value for $x = 0.0075$. So it is expected that the B-site cation is fully ordered for the complex perovskite composition $Ba_{0.9925}(Mg_{0.33}Ta_{0.67})O_3$. As a general rule, the increase of deviation from the ideal stoichiometry would cause an increase of the volume of the unit cell in complex perovskites.

Table 1. Unit Cell Parameters of $Ba(Mg_{0.33-x}Ta_{0.67})O_3$ and $Ba_{1-x}(Mg_{0.33}Ta_{0.67})O_3$ for Different Values of x[a]

	$Ba(Mg_{0.33-x}Ta_{0.67})O_3$			$Ba_{1-x}(Mg_{0.33}Ta_{0.67})O_3$		
x	a (Å)	c (Å)	c/a	a (Å)	c (Å)	c/a
−0.0150	5.7814	7.0678	1.2225	5.7832	7.0711	1.2226
−0.0100	5.7819	7.0680	1.2224	5.7821	7.0709	1.2228
−0.0050	5.7821	7.0671	1.2222	5.7810	7.0714	1.2232
0.0000	5.7720	7.0699	1.2249	5.7720	7.0699	1.2249
0.0025				5.7724	7.0711	1.2249
0.0050	5.7802	7.0799	1.2249	5.7757	7.0800	1.2258
0.0075				5.7749	7.0802	1.2260
0.0100	5.7818	7.0811	1.2247	5.7788	7.0784	1.2248
0.0150	5.7818	7.0845	1.2252	5.7799	7.0780	1.2246
0.0200	5.7820	7.0849	1.2252	5.7805	7.0762	1.2241
0.0250	5.7824	7.0833	1.2249	5.7823	7.0771	1.2233
0.0300	5.7835	7.0821	1.2245	5.7819	7.0691	1.2226

[a] The uncertainties in the determination of lattice parameters are between ±0.0001 and ±0.0003.

Microwave Dielectric Properties. The variation of the dielectric constant and τ_f with x in $Ba(Mg_{0.33-x}Ta_{0.67})O_3$ is plotted in Figure 7. The dielectric constant steadily increases as the magnesium deficiency increases. The increase in ϵ_r is

(35) Kim, E. S.; Yoon, K. H. *Ferroelectrics* **1992**, *133*, 187.

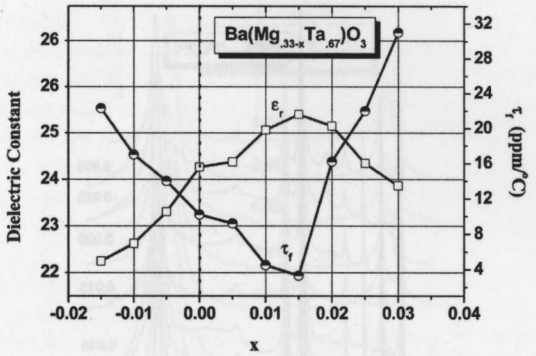

Figure 7. Variation of dielectric constant and temperature coefficient of resonant frequency of $Ba(Mg_{0.33-x}Ta_{0.67})O_3$, vs x.

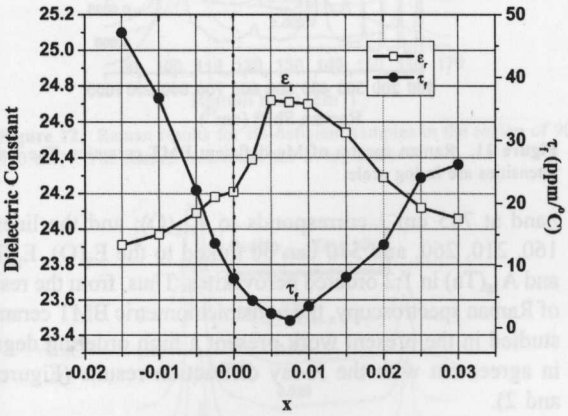

Figure 8. Variation of dielectric constant and temperature coefficient of resonant frequency of $Ba_{1-x}(Mg_{0.33}Ta_{0.67})O_3$, vs x.

in agreement with the increase in bulk density as shown in Figure 1. The presence of porosity decreases the dielectric constant since ϵ_r of air is unity. The magnesium deficiency resulted in enhanced material transport and densification, which is understood to be the reason for the increase of dielectric constant in the region $0.0 \leq x \leq 0.015$. For $x > 0.015$, the dielectric constant decreases further due to the appearance of the $Ba_5Ta_4O_{15}$ secondary phase, whose presence has been confirmed through XRD technique. It must be noted that adding an excess of MgO resulted in the decrease of the dielectric constant, which is due to the liquid-phase sintering and precipitation of MgO on the surface of BMT grains (see Figure 4b). The temperature coefficient of resonant frequency (τ_f) is 8 ppm/°C for the stoichiometric composition $Ba(Mg_{0.33}Ta_{0.67})O_3$ sintered at 1600 °C/(4 h) (see Figure 7). It approaches a minimum value of 4.2 ppm/°C for $x = 0.015$ in $Ba(Mg_{0.33-x}Ta_{0.67})O_3$. As the value of x increases further, τ_f also increases. For $x = 0.03$ the value of τ_f increased to 31 ppm/°C. The addition of an excess amount of MgO also results in the increase of τ_f. The variation of the temperature coefficient suggests that higher τ_f values are a consequence of greater lattice distortion.

The variation of dielectric constant and temperature coefficient of resonant frequency of Ba-deficient BMT samples are given in Figure 8. It is clear that the dielectric constant of the specimens increases with slight barium nonstoichiometry. The largest dielectric constant ($\epsilon_r = 24.7$) was measured for the $x = 0.005$ for the Ba-deficient sample.

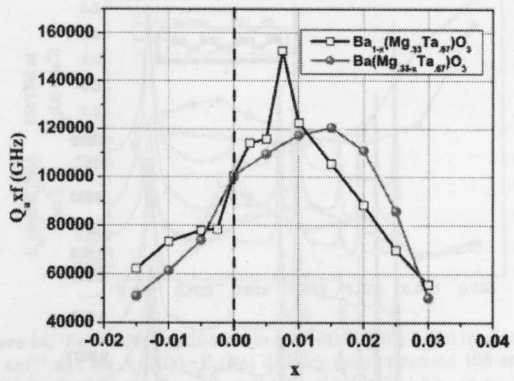

Figure 9. Variation of unloaded quality factor of $Ba(Mg_{0.33-x}Ta_{0.67})O_3$ and $Ba_{1-x}(Mg_{0.33}T_{0.67})O_3$, vs x.

For the stoichiometric BMT, this value was 24.2, while that for the highest level of nonstoichiometry ($x = 0.03$ in $Ba_{1-x}(Mg_{0.33}Ta_{0.67})O_3$) is 24.0. As seen from Figure 8, the decrease of the dielectric constant for Ba-rich specimens is mainly due to poor densification (see Figure 2). It is interesting to note that the temperature coefficient of resonant frequency of Ba-deficient samples first decreases and reaches a minimum of 1.2 ppm/°C for $x = 0.0075$ in $Ba_{1-x}(Mg_{0.33}Ta_{0.67})O_3$. The τ_f of Ba-excess BMT is increasing rapidly: for $x = -0.015$, τ_f is 47.1 ppm/°C.

The microwave quality factors of barium and magnesium nonstoichiometric BMT samples are given in Figure 9. A slight nonstoichiometry may be beneficial for enhanced material transport. The extensive deviation from stoichiometry and the associated point defects in complex perovskite $Ba(Mg_{0.33}Ta_{0.67})O_3$ can give rise to additional losses in BMT. Rong et al.[36] emphasized that the major cause for dielectric loss in complex perovskites is the enhanced concentration of point defects. The Q_uxf of pure stoichiometric BMT is 100 500 GHz. For a slight decrease of Mg concentration ($x = 0.015$ in $Ba(Mg_{0.33-x}Ta_{0.67})O_3$) the BMT ceramic observes a marginal increase in quality factor, as Q_uxf reaches 120 500 GHz. The Mg deficiency and excess Mg introduce a series of lattice defects in the crystal, apart from the distortion of the octahedral skeleton of oxygen. Consequently, the quality factor decreases. On the other hand, the unloaded quality factor increases with small percentages of Ba deficiency. The quality factor of $Ba_{0.9925}(Mg_{0.33}Ta_{0.67})O_3$ is $Q_uxf = 152\,580$ GHz. With further increase of x, the quality factor decreases, reaching $Q_uxf = 55\,570$ GHz for $x = 0.03$ in $Ba_{1-x}(Mg_{0.33}Ta_{0.67})O_3$. The quality factor of Ba-rich compositions is comparatively lower than that of Ba-deficient samples.

Raman Spectroscopy. The vibrational spectra of complex perovskite-type compounds are functions of both disordered and ordered regions with a particular symmetry, allowing the appearance of specific Raman scattering. Thus, in real systems, a combination of ordered and disordered regions makes the analysis of Raman data difficult in such materials.[37] The effects of ordering on the Raman spectra of

(36) Rong, G.; Newman, N.; Shaw, B.; Cronin, D. *J. Mater. Res.* **1999**, *14*, 4011.
(37) Moreira, R. L.; Matinaga, F. M.; Dias, A. *Appl. Phys. Lett.* **2001**, *78*, 428.

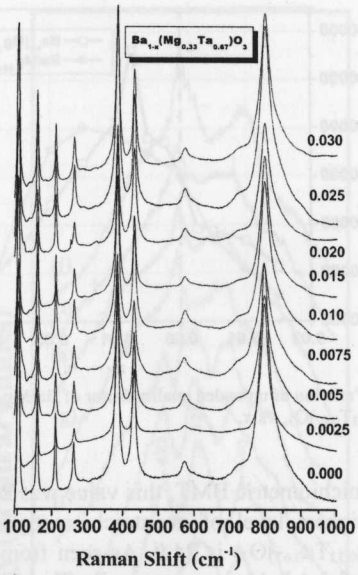

Figure 10. Raman spectra of Ba-deficient BMT ceramics. The Raman intensities are in log scale.

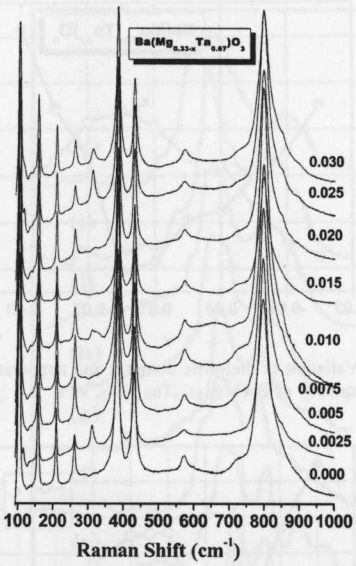

Figure 11. Raman spectra of Mg-deficient BMT ceramics. The Raman intensities are in log scale.

$Ba(Mg_{1/3}Ta_{2/3})O_3$ ceramics have been studied by a number of researchers.[38-40] Siny et al.[38,40] found that strong Raman lines were detected in BMT irrespective of whether 1:2 ordering was found by X-ray diffraction. According to these authors, if the Mg and Ta ions are randomly distributed, the structure should be a cubic perovskite with the space group $Pm3m$ (O_h^1), which has no Raman-active modes; 1:2 ordering distorts the structure to $P\bar{3}m1$ (D_{3d}^3), which gives $\Gamma_{Raman} = 4A_{1g} + 5E_g$, i.e., nine Raman-active modes. Siny et al.[38,40] attribute the four strong Raman lines to domains of 1:1 ordering with a superstructure, $Fm3m$ (O_h^5) symmetry, and $\Gamma_{Raman} = A_{1g} + E_g + 2F_{2g}$. These four lines occur in both 1:1 (PMT, PMN) and 1:2 (BZT, BMT) disordered structures. In the second case, three extra lines between 100 and 300 cm^{-1} were observed. These are particularly prominent in samples with high-Q values and may originate from the complete 1:2 order in the B sublattice, as a result of the $P\bar{3}m1$ space symmetry.

Figures 10 and 11 present the Raman spectra of Ba-deficient and Mg-deficient BMT ceramics, respectively. The intensities are in log scale to reveal details in the weaker lines, as well as the strongest ones. Apparently, the samples have a very good ordered structure because the Raman peaks are of narrow line width. As can be seen, four intense lines can be observed in all materials, together with three lines between 150 and 300 cm^{-1} and one broad line around 570 cm^{-1}, related to the 1:2 ordering in the B sublattice. The Raman phonon with the lowest energy near 105 cm^{-1} corresponds to the A_{1g}(Ba) and E_g(Ba) modes (the motion of Ba ions against the oxygen octahedral); the bands at about 380 and 430 cm^{-1} are associated with internal vibrations of oxygen octahedra, A_{1g}(O) and $2E_g$(O), respectively; the broad band at 795 cm^{-1} corresponds to A_{1g}(O); and the lines at 160, 210, 260, and 570 can be linked to the E_g(O), E_g(Ta), and A_{1g}(Ta) in 1:2 ordered perovskites. Thus, from the results of Raman spectroscopy, the nonstoichiometric BMT ceramics studied in the present work present a high ordering degree, in agreement with the X-ray diffraction results (Figures 1 and 2).

We now consider the effects of the nonstoichiometry on our Raman spectra. The spectra of Ba-deficient BMT ceramics look very similar (Figure 10), with few important differences in samples with $x = 0.0075$ and $x \geq 0.02$. For the first sample, a broad band at 120 cm^{-1} appeared, while bands around 312 cm^{-1} can be seen for $x \geq 0.02$. These extra lines can be associated with lattice distortions due to ordering for Ba-deficient ceramics and to the presence of second phases ($MgTa_2O_6$) detected by X-ray diffraction for $x \geq 0.02$ (Figure 3). The region of the spectra between 90 and 170 cm^{-1} was carefully studied in order to understand the influence of nonstoichiometry in the Raman scattering of Ba-deficient ceramics. The results are displayed in Figure 10, where it can be seen in detail the broad line at 120 cm^{-1} for $x = 0.0075$ in $Ba_{1-x}(Mg_{0.33}Ta_{0.67})O_3$ and the splitting in the lowest energy modes A_{1g}(Ba) and E_g(Ba) at 103 and 106 cm^{-1}, commonly observed as a single band.

For Mg-deficient samples (Figure 13) present extra weak lines at 112 and 118 cm^{-1} and a strong extra line at 313 cm^{-1} for $x = 0.0025$, a very low magnesium deficiency. Increasing the Mg deficiency, the extra bands tend to vanish for $x < 0.015$; at this value, the spectra are almost identical to the stoichiometric BMT. For deficiencies higher than 0.020, the bands appear probably due to distortions from the second phases $Ba_5Ta_4O_{15}$ and $BaTa_2O_6$ verified by X-ray diffraction (Figure 3). In Ba-deficient samples (see Figure 12), the region 90−170 cm^{-1}, as depicted in Figure 13 for all Mg-deficient ceramics, shows the splitting of the A_{1g}-(Ba) and E_g(Ba) modes together with the extra lines at 112 and 118 cm^{-1} for $x = 0.0025$ and weak bands at 118 cm^{-1} for $x \geq 0.02$.

(38) Siny, I. G.; Tao, R.; Katiyar, R. S.; Guo, R.; Bhalla, A. S. *J. Phys. Chem. Solids* **1998**, *59*, 181.
(39) Ravichandran, D.; Jin, B.; Roy, R.; Bhalla, A. S. *Mater. Lett.* **1995**, *25*, 257.
(40) Siny, I. G.; Katiyar, R. S.; Bhalla, A. S. *J. Raman Spectrosc.* **1998**, *29*, 385.

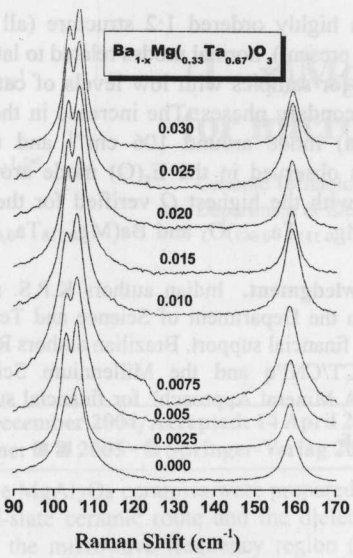

Figure 12. Raman results for Ba-deficient samples in the region of 90–170 cm^{-1}. The Raman intensities are in log scale.

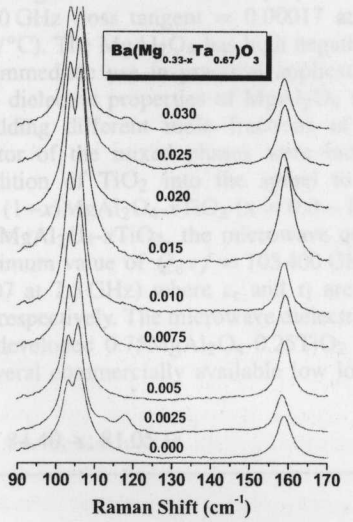

Figure 13. Raman results for Mg-deficient samples in the region of 90–170 cm^{-1}. The Raman intensities are in log scale.

The variations of Raman lines and the full width at half-maximum (fwhm) are important fingerprints to study the phonons in samples with different compositions, particularly those related to cation deficiency. These nonstoichiometric samples present ion movements that lead to lattice distortions, which can be observed by Raman spectroscopy. In this work, Raman modes and fwhm for all bands associated with the normal modes of oxygen and barium were investigated in detail. Vibrations associated with Ta atomic motion are expected to show relatively small changes or to be quasi-invariant. Figure 14 presents the fwhm for the band at 157 cm^{-1}, $E_g(O)$ mode, which showed a pronounced variation with nonstoichiometry. Also, the difference between the frequencies for the $A_{1g}(Ba)$ and $E_g(Ba)$ modes is plotted for all samples. It was verified that the fwhm increased for $x < 0.0075$ in Ba-deficient ceramics, decreasing in more cation deficient samples. The huge increase of fwhm for the materials with lower Ba contents ($x = 0.025$ and 0.030) can

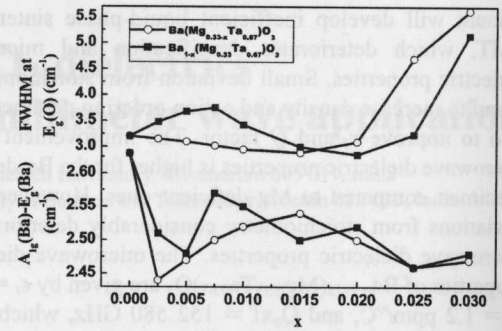

Figure 14. Full width at half-maximum (fwhm) of the $E_g(O)$ mode around 157 cm^{-1} and the $A_{1g}(Ba)-E_g(Ba)$ distance (modes around 106 and 103 cm^{-1}), for $Ba(Mg_{0.33-x}Ta_{0.67})O_3$ and $Ba_{1-x}(Mg_{0.33}Ta_{0.67})O_3$, vs x.

be related to the presence of a secondary phase ($MgTa_2O_6$). Conversely, Mg-deficient ceramics exhibit a decreasing tendency of fwhm of this mode with nonstoichiometry until $x < 0.015$, followed by increasing due to the secondary phases $Ba_5Ta_4O_{15}$ and $BaTa_2O_6$. Raman splitting observed for the lowest frequency $A_{1g}(Ba)$ and $E_g(Ba)$ bands (around 105 cm^{-1}) presented a curious behavior. Considering only the nonstoichiometric samples, we note that a maximum difference between the frequencies of these bands is observed at $x = 0.0075$ in Ba-deficient samples and at $x = 0.015$ in Mg-deficient materials.

Raman results can be now correlated to the microwave properties of the nonstoichiometric BMT ceramics. The compositions $Ba_{0.9925}(Mg_{0.333}Ta_{0.667})O_3$ and $Ba(Mg_{0.318}Ta_{0.667})O_3$ showed the highest ordering degree and the more pronounced splitting of the (422) and (226) diffraction lines from all samples studied. This result is indicative of the lattice distortion caused by the cation deficiency. Also, these BMT compounds showed maximum values of dielectric constant, quality factor, and τ_f close to zero. Thus, nonstoichiometry showed advantages in terms of the microwave properties. Raman analysis verified evidences of lattice distortion in both Ba- and Mg-deficient ceramics. According to Kawashima,[6] the nonstoichiometry leads to an increase in the degree of 1:1 B-site ordering. However, in the present work, the modes associated with the 1:1 ordered phase do not present significant change.

Conclusions

The complex relationship between stoichiometry and microwave loss quality of complex perovskite $Ba(Mg_{1/3}Ta_{2/3})O_3$ ceramics was investigated. The influence of A- and B-site cation nonstoichiometry on the sinterability and microwave dielectric properties of low-loss ceramic barium magnesium tantalate is explored by intentionally altering the barium and magnesium ion concentrations. It is found that density increases with slight nonstoichiometry ($x = 0.015$) of Mg^{2+} concentration, which is caused by enhanced material transport due to vacancies. The cation ordering between Mg^{2+} and Ta^{5+} ions reaches a maximum for $x = 0.015$ in $Ba(Mg_{0.33}Ta_{0.67})O_3$ which shows better microwave dielectric properties [$\epsilon_r = 25.1$, $\tau_f = 3.3$ ppm/°C, and $Q_u xf = 120\,500$ GHz] compared to stoichiometric BMT [$\epsilon_r = 24.2$, $\tau_f = 8$ ppm/°C, $Q_u xf = 100\,500$. The addition of MgO in a large excess

amount will develop inefficient liquid-phase sintering of BMT, which deteriorates densification and microwave dielectric properties. Small deviation from stoichiometry is found to increase density and cation ordering parameter and also to improve τ_f and Q factor. The improvement of the microwave dielectric properties is higher for the Ba-deficient specimen compared to Mg-deficient ones. However, large deviations from stoichiometry considerably deteriorate the microwave dielectric properties. The microwave dielectric properties of $Ba_{0.9925}(Mg_{0.33}Ta_{0.67})O_3$ are given by $\epsilon_r = 24.7$, $\tau_f = 1.2$ ppm/°C, and $Q_u xf = 152\,580$ GHz, which is the best among the nonstoichiometric samples studied in this investigation. Variations in Raman spectra of nonstoichiometric BMT ceramics were described and correlated to changes in the nature of cation ordering. Although the results showed a highly ordered 1:2 structure (all Raman-active bands are present), normal modes related to lattice distortions appeared for samples with low levels of cation deficiency and/or secondary phases. The increase in the frequency of the E_g(Ba) mode around 106 cm^{-1} and the bandwidth variations observed in the E_g(O) mode around 157 cm^{-1} coincide with the highest Q verified for the compositions $Ba_{0.9925}(Mg_{0.333}Ta_{0.667})O_3$ and $Ba(Mg_{0.318}Ta_{0.667})O_3$.

Acknowledgment. Indian authors K.P.S. and M.T.S. are grateful to the Department of Science and Technology, New Delhi, for financial support. Brazilian authors R.L.M. and A.D. thank MCT/CNPq and the Millennium Science Initiative "Water: A Mineral Approach" for financial support.

CM048411S